

International Atomic Energy Agency

INDC(CCP)-154/L

---

**INDC**

**INTERNATIONAL NUCLEAR DATA COMMITTEE**

---

Investigations of the Interactions of  
Neutrons with  $^{238}\text{U}$  Nuclei

B.V. Zhuravlev, L.E. Kazakov, V.N. Kononov,  
N.V. Kornilov, B.D. Kuz'minov, V.V. Malinovskij,  
E.D. Poletaev, O.D. Sal'nikov and N.N. Semenova

Institute of Physics and Power Engineering, Obninsk, USSR

Translated by the IAEA  
August 1980

---

**IAEA NUCLEAR DATA SECTION, WAGRAMERSTRASSE 5, A-1400 VIENNA**

Reproduced by the IAEA in Austria  
August 1980  
80-4004

Investigations of the Interactions of  
Neutrons with  $^{238}\text{U}$  Nuclei

B.V. Zhuravlev, L.E. Kazakov, V.N. Kononov,  
N.V. Kornilov, B.D. Kuz'minov, V.V. Malinovskij,  
E.D. Poletaev, O.D. Sal'nikov and N.N. Semenova

Institute of Physics and Power Engineering, Obninsk, USSR



INVESTIGATIONS OF THE INTERACTIONS OF  
NEUTRONS WITH  $^{238}\text{U}$  NUCLEI

B.V. Zhuravlev, L.E. Kazakov, V.N. Kononov,  
N.V. Kornilov, B.D. Kuz'minov, V.V. Malinovskij,  
E.D. Poletaev, O.D. Sal'nikov and N.N. Semenova

Institute of Physics and Power Engineering, Obninsk, USSR

Uranium-238 is the main raw material used in nuclear power engineering. It is necessary to study the interactions of neutrons with uranium-238 nuclei from all points of view because of the varied role of this material in fast neutron reactors. Radiative capture of neutrons by uranium-238 has as its final result the formation of plutonium-239 nuclei. The extent of participation in the fission chain reaction depends on the fission cross-section and on the number and spectrum of the secondary neutrons emitted. Because of the high proportion of uranium nuclei in the core and blanket zone in fast neutron reactors, the capacity of uranium-238 nuclei to scatter neutrons elastically and inelastically has a considerable influence on the shape of the neutron spectrum of the reactor. In addition, the  $(n,2n)$  reaction with uranium-238 is the first step in the chain of nuclear transformations leading to an accumulation in the fuel and raw materials of the light isotope uranium-232, which causes serious difficulties in the external fuel cycle.

So far these reactions have not been studied sufficiently consistently in a wide range of neutron energies which includes the fission neutron spectrum. The present paper reviews a number of experimental investigations of the interaction of neutrons with uranium-238 nuclei performed at the Institute of Physics and Power Engineering.

#### I. MEASUREMENTS OF THE AVERAGE NUMBER OF PROMPT NEUTRONS WITH FISSION OF URANIUM-238 NUCLEI BY NEUTRONS

For fission of uranium-238 nuclei by neutrons, measurements of  $\bar{\nu}_p$  were performed relative to  $\bar{\nu}_p = 3.733$  for spontaneous fission of  $^{252}\text{Cf}$  nuclei. Detailed descriptions of the measurement method are given in other papers. Here we shall merely mention some of its special features concerning  $^{238}\text{U}$  measurements. The ionization chamber, containing uranium-238 foils with a total weight of 0.76 g, consisted of six sections. For this work uranium-238 with an enrichment of 99.999% was used. The foil thickness was approximately

$1 \text{ mg} \cdot \text{cm}^{-2}$ . The efficiency of fission fragment detection was in the region of 90%. The possibility of increasing it further is limited because of the counting of alpha-particles in the fission fragment detection channel. Monoenergetic neutrons were obtained in the T(p,n) and D(d,n) reactions. The neutron background arising as a result of the interaction of deuterons with the target backing material and with implanted deuterons was taken into account by performing measurements with a blank target without an adsorbed deuterium foil. The number of fission events of uranium-238 nuclei caused by background neutrons did not exceed 10% when using a fresh target for 12 hours.

Table 1 shows a list of corrections (%) and the contributions of uncertainties in them to the total error in determining  $\bar{v}_p$ . Corrections in  $\delta$  take into account the following effects: the difference in energy spectra of fission neutrons ( $\delta_1$ ); the dependence of the efficiency of neutron detection on the position on the detector axis ( $\delta_2$ ); the difference in the foil diameters of  $^{238}\text{U}$  and  $^{252}\text{Cf}$  ( $\delta_3$ ); miscalculations as a result of coincidence within dead-time limits of pulses from fission neutrons ( $\delta_4$ ); miscalculations as a result of coincidence within dead-time limits of a fission neutron pulse and a background pulse ( $\delta_5$ ); discrimination in the fission fragment channel ( $\delta_6$ ); the difference in the layer thicknesses of  $^{238}\text{U}$  and  $^{252}\text{Cf}$  ( $\delta_7$ ); spontaneous fission of uranium-238 and alpha-particle pulse pile-up count ( $\delta_8$ ); angular anisotropy of fission fragments ( $\delta_9$ ); and background neutrons where the D(d,n) reaction is used ( $\delta_{10}$ ).

The statistical error in measurements was approximately 0.5%.

The measurements are shown in Table 2.

## II. URANIUM-238 FISSION NEUTRON SPECTRA

The uranium-238 fission neutron spectra were measured by the time-of-flight method in a range of bombarding neutron energies of 6-16 MeV. For detection of the fission events a multi-section fission chamber containing 2.47 g uranium-238 was used. The efficiency of detection of fission events was 75%.

A neutron detector based on a stilbene crystal and an FEhU-30 photo-multiplier with gamma-ray compensation was placed in a shield with a collimator at a distance of 1.9 m from the fission chamber and at an angle of 90° to the

axis of the accelerated particles. The efficiency of the detector was determined from the spectrum of californium-252 fission neutrons, the Maxwellian parameter  $T$  having been taken to be 1.42 MeV. The surface of the ionization chamber electrodes was positioned perpendicular to the direction of flight of the neutrons being detected. By means of this geometry it was easy to make a correction for attenuation and multiple scattering of fission neutrons in the chamber. This correction amounted to 1-2% for the whole secondary neutron energy range (0.6-8 MeV). Aspects of the method used are examined in greater detail in Ref. [1].

Neutrons with an energy of 14.3 MeV were produced on a KG-0.25 accelerator in the  $T(d,n)$  reaction and 6-9 MeV neutrons on an EhGP-10M accelerator in the  $D(d,n)$  reaction. In the latter case a gaseous deuterium target was used. The time resolution was 1.5-2 ns/m. The contribution of background neutrons from target structures did not exceed 5% ( $E_n = 9$  MeV).

In this study absolute spectra (neutron/fission MeV) were obtained for the primary neutron energies 6, 7, 8, 9 and 14.3 MeV.

All the spectra with  $E_n > E_0 - B_F$  ( $E_0$  is the energy of bombarding neutrons and  $B_F$  is the threshold of the  $(n,n'f)$  reaction) are well described by a Maxwellian distribution (Fig. 1). Values of  $T(E_0)$  obtained by the least-squares method are shown in Table 3. This table also shows values for  $\bar{\nu}(E_0)$  - the average number of prompt neutrons for fission events which are not preceded by the emission of inelastically scattered neutrons. When obtaining  $\bar{\nu}(E_0)$  account was taken of the angular anisotropy of the neutrons detected (approximately 10%), which was due partly to the effect of collimating neutrons by discrimination in the fission fragment recording channel and partly to the angular anisotropy of the fission fragments.

For explaining the dependence  $T(E_0)$  obtained, a calculation was performed on the basis of the following assumptions:

1. Where  $E_0 < B_F$  the parameter  $T$  was described by the Terrel ratio

$$T = a + b \sqrt{\nu + 1}$$

The data in the literature for  $T$  for various fissionable nuclei in the case of  $E_0 < B_F$  were analysed. The following results were obtained:

$$a = 0.41, \quad b = 0.47.$$

2. The total number of prompt neutrons is

$$\bar{\nu} = \sigma_0 \bar{\nu}_0 + \sigma_1 (\bar{\nu}_1 + 1) + \sigma_2 (\bar{\nu} + 2)$$

where  $\sigma_i$  is the proportion of fission events with previous emission of  $i$  neutrons and  $\bar{\nu}_i$  is the number of fission neutrons after emission of  $i$  neutrons. Making the assumption that the energy dependence  $\bar{\nu}_0(E_0)$  for  $E_0 < B_F$  can be extrapolated to the energy region  $E_0 > B_F$  and taking given values for  $\sigma_i$ , it is possible to find  $\bar{\nu}_i(E)$  and to calculate  $T_i$ . Since the values of  $T_i$  are close to each other, the sum of the Maxwellian distributions can be replaced by a single Maxwellian distribution with the parameter  $\bar{T}$ :

$$\bar{T} = \frac{\sum \sigma_i \nu_i T_i}{\sum \sigma_i \nu_i}$$

Figure 2 shows the dependence  $\bar{T}(E)$  obtained in this way together with experimental results from the work described in the present paper and data from other papers. The calculated values for  $\bar{T}(E)$  agree well with the experimental data. The systematic increase in measurements where  $E_0 \approx 14$  MeV is associated with the considerable contribution of direct processes to the spectrum of previously emitted neutrons where  $E_n > 3$  MeV, i.e. to the energy region in which the parameter  $T$  is determined.

### III. THE SPECTRA OF NEUTRONS INELASTICALLY SCATTERED BY URANIUM-238 NUCLEI

The total spectra of secondary neutrons formed in the interaction of 6-9 MeV neutrons with uranium-238 nuclei were measured by the time-of-flight method on the spectrometer of an EhGP-10M accelerator.

A gaseous deuterium target was used as the neutron source. The time resolution was 1.5 ns/m. At neutron energies of 9 MeV account was taken of the background from the deuteron decay reaction  $D(d, np)$ . The specimen used was a hollow cylinder of metallic uranium-238 ( $H = 49$  mm,  $R_1 = 22.6$  mm,  $R_2 = 19.9$  mm). The correction for multiple scattering and attenuation of the neutron flux was determined experimentally and compared with calculation. Satisfactory agreement was obtained. For  $E_0 = 6$  and 8 MeV the angular distributions of neutrons were measured. In other cases the spectra were measured only at  $90^\circ$ . After calculation of the fission neutron spectra the neutron spectra from the  $(n, 2n)$  and  $(n, n')$  reactions were found. On the basis of experimental cross-sections of the  $(n, 2n)$  reaction and the evaluated



shape of the second neutron spectrum from the  $(n,2n)$  reaction it is possible to find the spectrum of the first neutron. Analysis of the results shows that in order to describe the spectra in a wide energy range it is necessary to use two reaction mechanisms - the equilibrium and direct mechanisms (Fig. 3). The first process accounts for up to 30% ( $E_0 = 8$  MeV) where angular anisotropy is insignificant. The derived level density parameter is constant where the initial energy varies from 6 to 9 MeV. The mean value of  $\bar{a} = 32.6$  MeV<sup>-1</sup> is in good agreement with resonance data.

#### IV. MEASUREMENTS OF THE ENERGY DEPENDENCE OF THE $^{238}\text{U}(n,2n)$ REACTION CROSS-SECTION

The  $^{238}\text{U}(n,2n)$  reaction cross-section was measured by the activation method in a neutron energy range of 6.5-10.5 MeV. The neutron source used was a gaseous deuterium target mounted on an EhGP-10M accelerator. The neutron flux density was measured in relation to the  $^{238}\text{U}(n,f)$ ,  $^{27}\text{Al}(n,\alpha)$  and  $^{56}\text{Fe}(n,p)$  reactions.

Table 4 shows the  $^{238}\text{U}(n,2n)$  reaction cross-sections obtained. In Fig. 4 the measured  $^{238}\text{U}(n,2n)$  reaction cross-sections are compared with those obtained by different groups of experimenters.

The methods used for performing measurements, the experimental results and their accuracy are discussed in greater detail in Ref. [2].

#### V. RADIATIVE CAPTURE OF NEUTRONS BY URANIUM-238 NUCLEI

An absolute method of measuring the cross-section for radiative capture of neutrons by uranium-238 nuclei in the energy region 10-500 keV has been developed. This method of measuring the neutron capture cross-section involves the use of a large liquid scintillation detector for recording capture events on the basis of prompt gamma quanta and nanosecond time-of-flight technology with an electrostatic pulse generator. Unlike traditional capture cross-section measurements on similar spectrometers involving relative methods, because of the possibility of obtaining a resonance neutron spectrometer regime on the EhG-1 FEhI accelerator, for the purposes of this experiment use was made of the "saturated resonance" method, by means of which it was possible to dispense with direct measurement of the efficiency of the capture event detector and absolute measurement of the neutron flux. In addition, the "amplitude weighting" method was used, which made it possible to reduce the error associated with the sensitivity of the detector to

possible changes in the spectrum and to the multiplicity of capture gamma quanta with the transition from saturated S-resonance ( $E_0 = 6.67$  eV) to fast neutrons and also to extend the measurement technique to nuclei which do not have resonances that are convenient for normalization.

Fast and resonance neutrons were measured on a spectrometer based on an EhG-1 FEH1 pulse accelerator with which it was possible to obtain pulses in both the nanosecond and microsecond ranges. The parameters of the proton beam on the target when operating in the fast neutron region were as follows: duration 3-6 ns, amplitude 1.5 mA and repetition interval 2.8  $\mu$ s. For operation in the resonance region the duration was 0.5  $\mu$ s, the amplitude 0.35 mA and the repetition interval 140  $\mu$ s. For a neutron source the  ${}^7\text{Li}(p,n)$  reaction and a "thick" metallic lithium target were used. For work in the resonance neutron spectrometer regime, a polyethylene moderator was installed for shaping the resonance neutron flux near the target, Cd and In filters being used to remove recycled neutrons.

Figure 5 shows a block diagram for the experimental device used. The capture event detector is a spherical scintillation tank with a capacity of 17 l. A scintillator based on hexafluorobenzene and also on toluene with the addition of 60% trimethyl borate was used. The neutron flux was monitored during measurement in the energy region up to 100 keV by a detector based on thin (0.8 mm)  ${}^6\text{Li}$  glass placed in front of the capture sample. A second detector consisting of a  ${}^{10}\text{B}$  sheet and two NaI(Tl) crystals monitored the flux at higher energies. The neutron beam was directed into the measuring area through a channel 40 mm in diameter within the 2-m concrete wall of the accelerator target room. By this means it was possible to make a radical improvement in the background of the experiment and to obtain a capture event and neutron flux detector background similar to that of the natural background.

Figure 6 shows typical recorded time-of-flight spectra obtained for the resonance neutron region.

Figure 7 shows measurements for  ${}^{137}\text{Cs}$  ( $E_0 = 5.9$  eV) where theoretical radiative capture probabilities, taking into account corrections for neutron absorption after scattering, are shown as a solid line.

Use of the amplitude weighting method requires, in addition, measurement of amplitude capture events and knowledge of the weighting function of the detector. Since for detectors of the large liquid scintillation type the

probability of simultaneous recording of several gamma quanta from one cascade of capture gamma rays is high, the weighting function  $G(U)$  cannot be determined unequivocally as, for example, in the case of detectors of small volume, and it becomes dependent on multiplicity. Model calculations have shown that the dependence of  $G(U)$  on multiplicity can decrease considerably where the total cascade energy  $B_n$  is included in the weighting function as a parameter.

As a result of performing measurements with samples of Ag, Sb, Cs, Sm, Hf, Ta, Au and  $^{238}\text{U}$  by the saturated resonance method for determining the absolute number of neutron capture events in a sample, the following weighting function for a scintillator based on toluene was obtained:

$$G(U) = 3,043 E_n^{-0,22} \cdot U^{1,75}$$

The error in determination of the normalization constant is 2%. For determining the error associated with the finite thickness of the samples studied, measurements were performed with various uranium sample thicknesses and also using metallic and oxide ( $\text{U}_3\text{O}_8$ ) samples. Figure 8 shows preliminary measurements of radiative capture cross-sections for  $^{238}\text{U}$  and  $^{197}\text{Au}$ .

The method used for measuring cross-sections of neutron radiative capture by uranium-238 in the energy range 0.35-1.4 MeV and the measurements themselves are given in detail in Ref. [3]. Samples were irradiated on an electrostatic accelerator using the  $\text{T}(p,n)$  and  $\text{D}(d,n)$  reactions. The neutron flux was recorded by means of a counter filled with hydrogen or methane. The sample activity was measured with a GeLi detector. The absolute activity was determined by the method of  $4\pi$   $\beta$ - $\gamma$  coincidences. The measurements are shown in Table 5.

REFERENCES

- [1] BARYBA, V.Ya., KORNILOV, N.V., SAL'NIKOV, O.A., "The uranium-238 prompt fission neutron spectrum at an energy of 14.3 MeV", preprint FEI-947, Obninsk (1979) [in Russian].
- [2] KORNILOV, N.V., et al., "Cross-section measurements for the  $^{238}\text{U}(n,2n)$  reaction from 6.5 to 10.5 MeV", International Symposium on Interaction of Fast Neutrons with Nuclei, Gaussig, German Democratic Republic (1979) [in Russian].
- [3] DAVLETSHIN, A.N., TIKHONOV, S.V., TIPUNKOV, A.O., TOLSTIKOV, V.A., At. Ehnerg. 48(2) (1980) 87 [in Russian].

Table 1

$\delta$	Correction (%)	Error	$\delta$	Correction (%)	Error
1	-(0,6 - 1,9)	$2^{\pm} 0,4$	6	+ 0,2	$\pm 0,1$
2	+ 4,6	$\pm 0,3$	7	+ 0,1	$\pm 0,3$
3	- 0,3	$\pm 0,2$	8	+(0,2 - 0,5)	$\pm 0,2$
4	+(0,9 - 1,8)	$\pm 0,2$	9	0,1	$\pm 0,1$
5	+ 0,1	$\pm 0,1$	10	+(1,0 - 1,2)	$\pm 0,1$

Table 2

$E_n$	$\pm \Delta E_n$	$\bar{V}_p$	$\pm \Delta V_p$	$E_n$	$\pm \Delta E_n$	$\bar{V}_p$	$\pm \Delta V_p$
1,30	0,05	2,431	0,048	2,60	0,03	2,638	0,025
1,40	0,05	2,458	0,045	2,70	0,03	2,661	0,028
1,50	0,04	2,473	0,027	2,80	0,03	2,687	0,020
1,60	0,04	2,533	0,026	2,90	0,04	2,693	0,023
1,70	0,04	2,510	0,035	3,00	0,04	2,683	0,023
1,75	0,05	2,610	0,023	3,10	0,04	2,693	0,026
1,80	0,04	2,537	0,026	3,20	0,04	2,735	0,023
1,90	0,04	2,547	0,025	3,30	0,04	2,765	0,023
2,00	0,04	2,565	0,022	3,40	0,03	2,745	0,026
2,10	0,04	2,613	0,031	3,50	0,03	2,735	0,023
2,20	0,03	2,625	0,025	3,60	0,03	2,803	0,029
2,30	0,03	2,655	0,022	3,70	0,03	2,790	0,026
2,40	0,03	2,587	0,022	5,58	0,08	3,151	0,058
2,50	0,03	2,632	0,022	5,89	0,07	3,219	0,031

Table 3

$E_0$ (MeV)	6	7	8	9	14,3
$T(E_0)$ (MeV)	$1,36^{\pm} 0,03$	$1,31^{\pm} 0,03$	$1,36^{\pm} 0,04$	$1,41^{\pm} 0,04$	$1,58^{\pm} 0,02$
$\gamma(E_0)$	$3,09^{\pm} 0,11$	$2,85^{\pm} 0,09$	$3,12^{\pm} 0,17$	$3,16^{\pm} 0,24$	

Table 4

E (MeV)	6,54	6,78	7,00	7,5	7,99	8,50	8,99	9,49	10,0	10,50
(n,2n)	72	251	402	831	1077	1244	1344	1371	1413	1466
mb	± 5	± 13	± 18	± 30	± 31	± 41	± 35	± 36	± 37	± 63

Table 5

Neutron energy (keV)	Radiative capture cross-section (mb)	Neutron energy (keV)	Radiative capture cross-section (mb)
348 ± 23	119,9 ± 2,8%	700 ± 41	128,8 ± 2,8%
348 ± 15	122,3 ± 3,0%	792 ± 22	135,7 ± 4,2%
350 ± 24	124,8 ± 2,8%	1026 ± 22	124,2 ± 3,6%
352 ± 25	117,4 ± 3,1%	1192 ± 33	87,4 ± 3,1%
590 ± 23	130,8 ± 3,6%	1400 ± 31	69,6 ± 3,0%
597 ± 16	127,1 ± 3,9%	1400 ± 31	75,9 ± 2,7%
600 ± 22	114,0 ± 2,5%	1400 ± 23	71,7 ± 2,5%
603 ± 36	114,6 ± 2,7%		

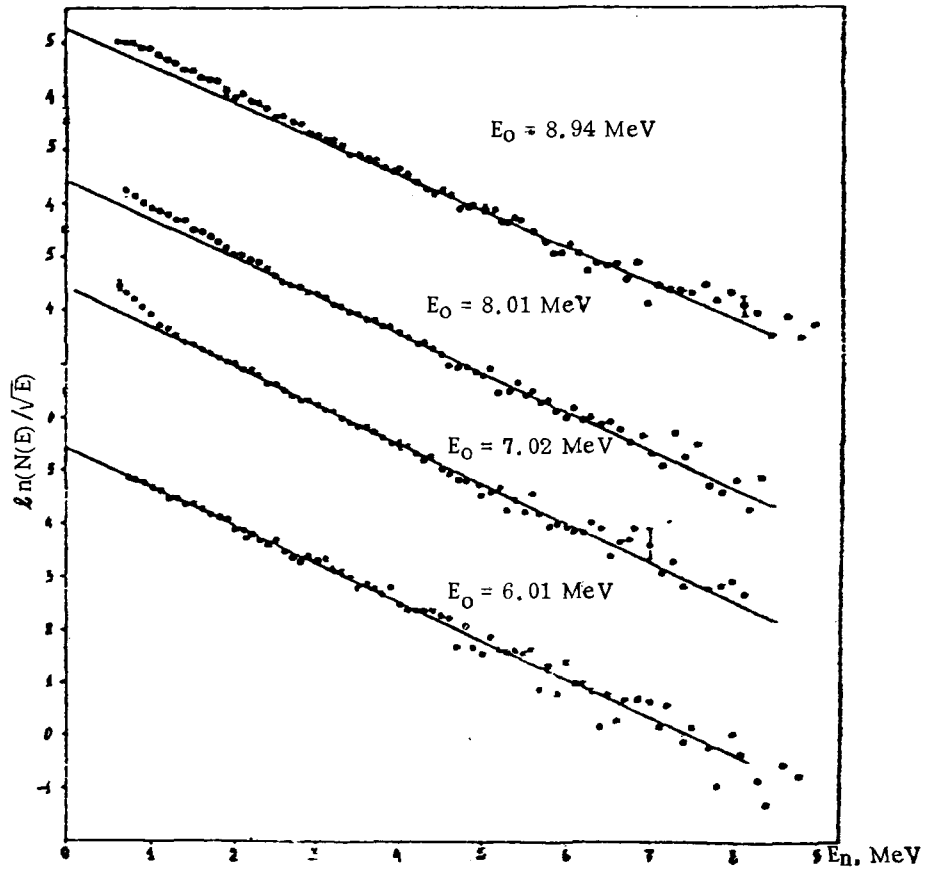
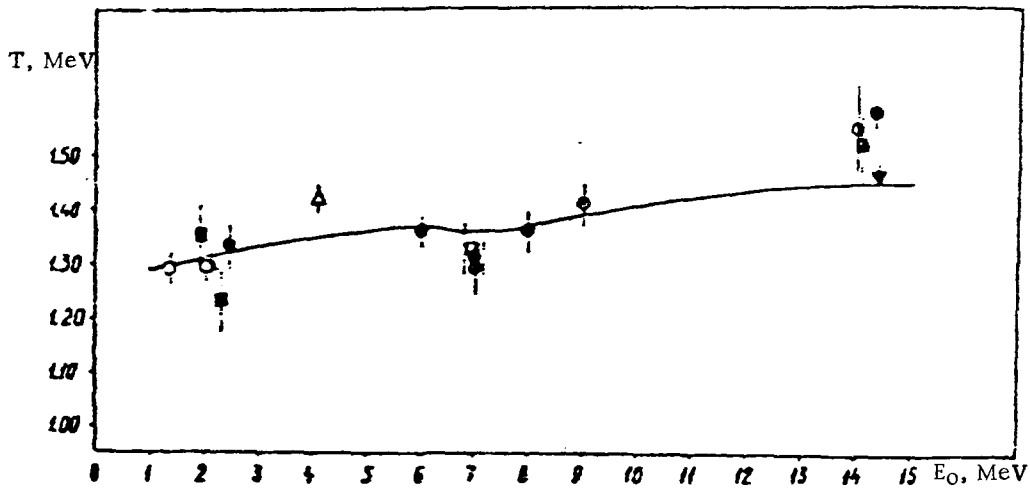
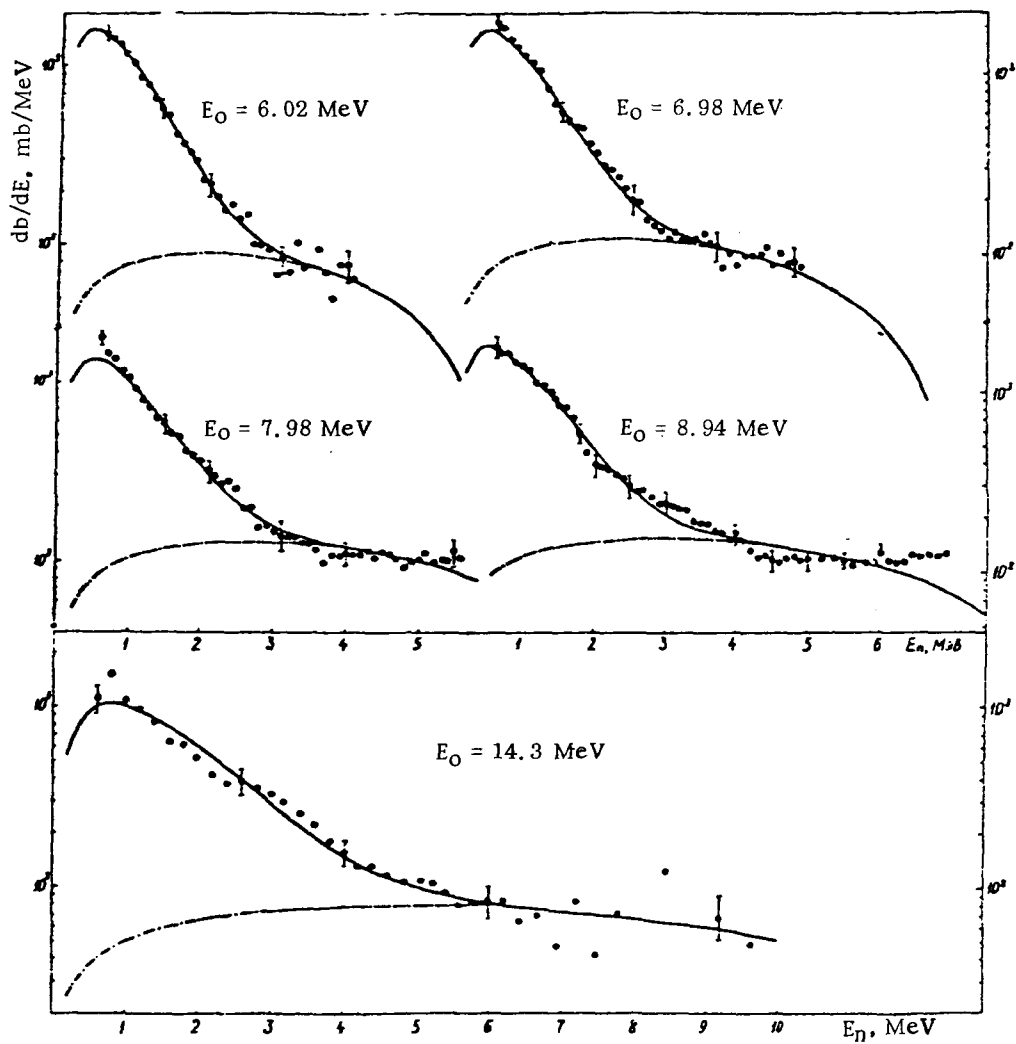


Fig. 1: Spectra of neutrons from fission of  $^{238}\text{U}$  nuclei by neutrons with energies of 6, 7, 8 and 9 MeV



**Fig. 2:** Energy dependence of the Maxwellian parameter ( $T$ ) describing the fission neutron spectra



**Fig. 3:** The spectra of neutrons inelastically scattered by  $^{238}\text{U}$  nuclei



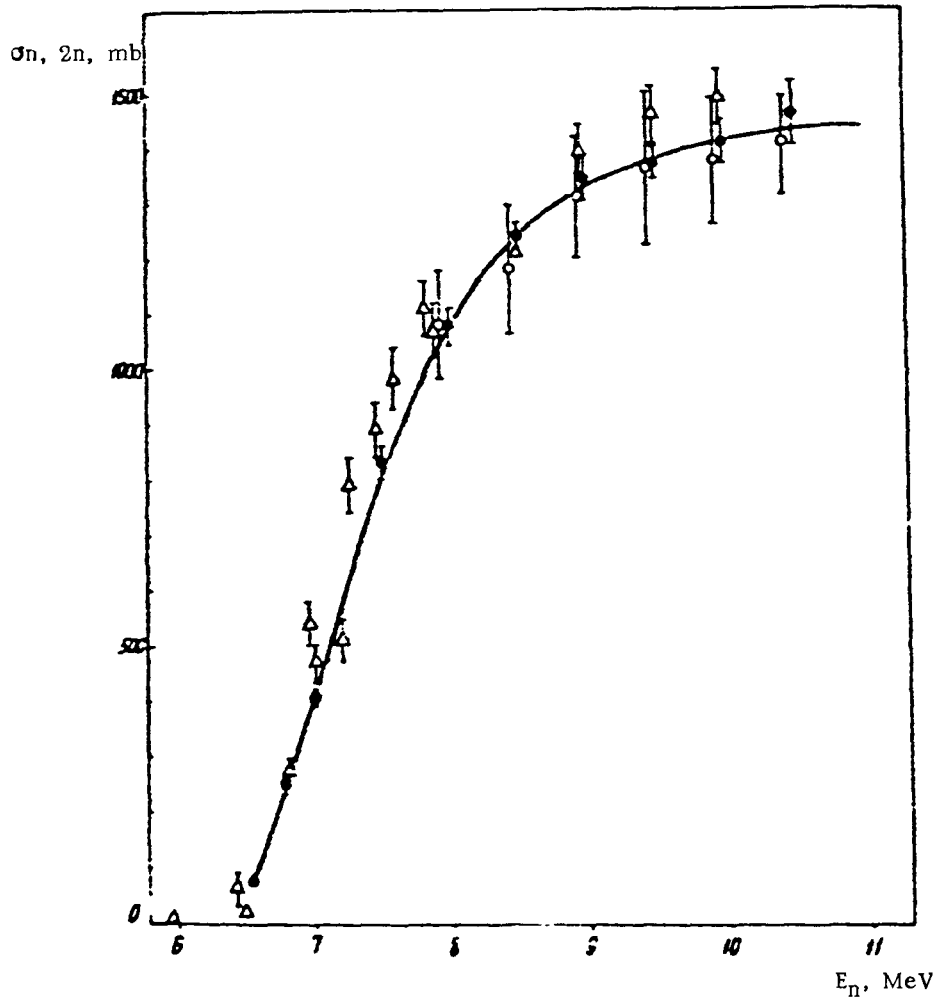


**Fig. 4:** Cross-section of the (n,2n) reaction for  $^{238}\text{U}$  nuclei; ● represents the results of the present study.

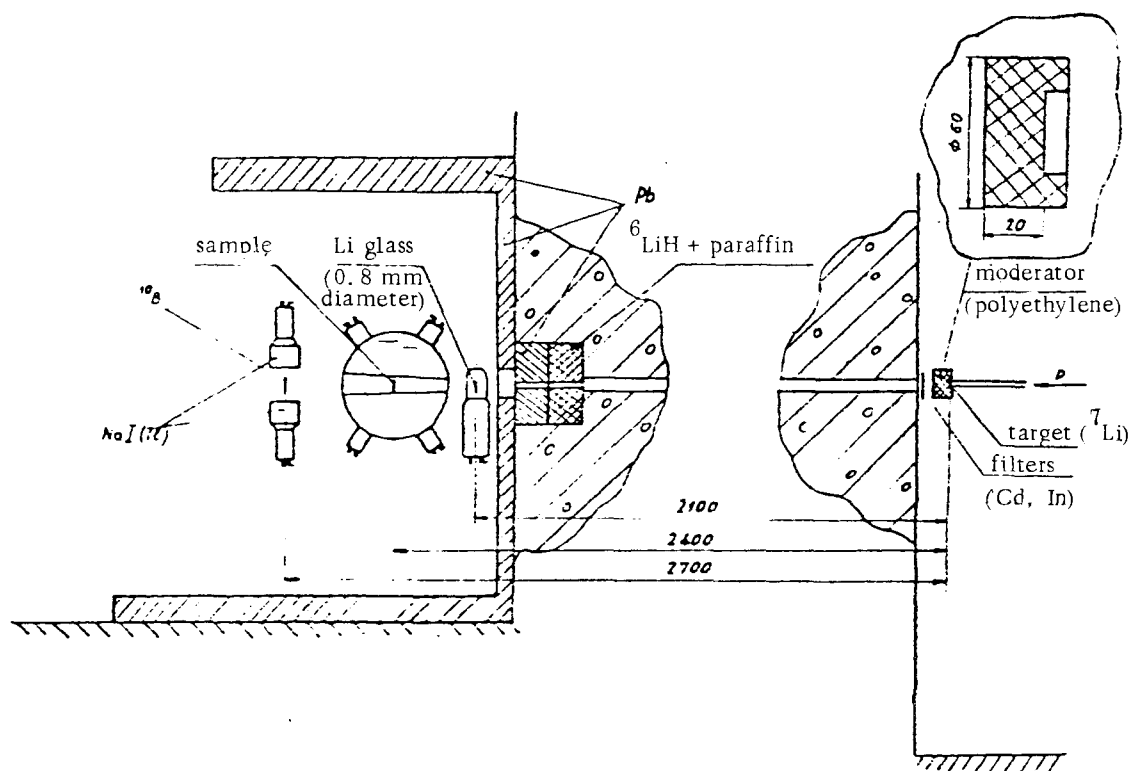


**Fig. 5:** Block diagram of experimental device for measuring neutron radiative capture cross-sections.

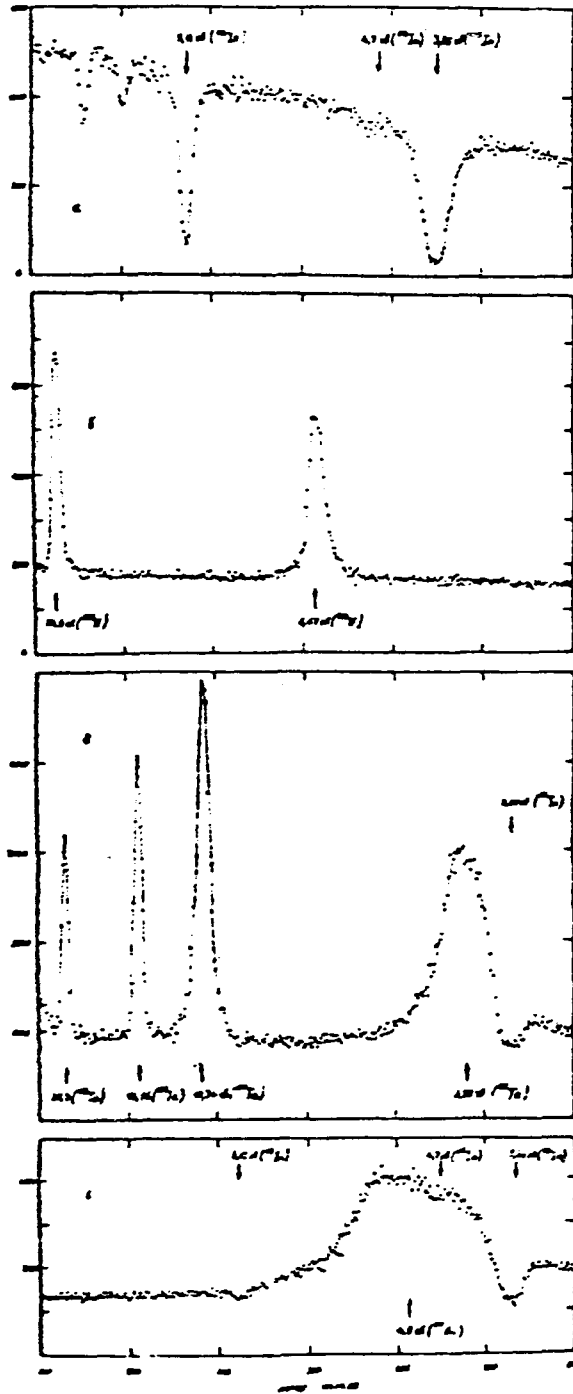


Fig. 6: Recorded time-of-flight spectra for the resonance neutron region

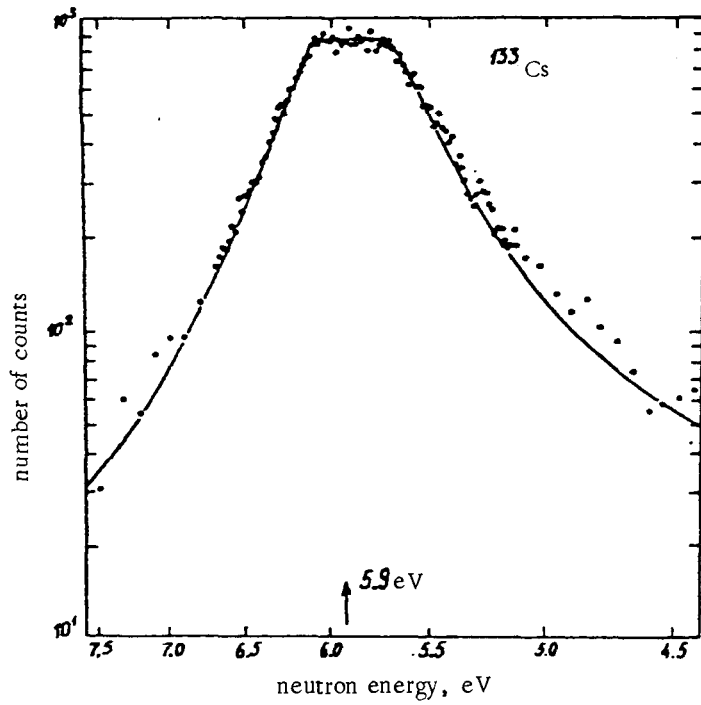


Fig. 7: Measurements for  $^{137}\text{Cs}$  in the absorbed-resonance region ( $E_0 = 5.9$  eV).

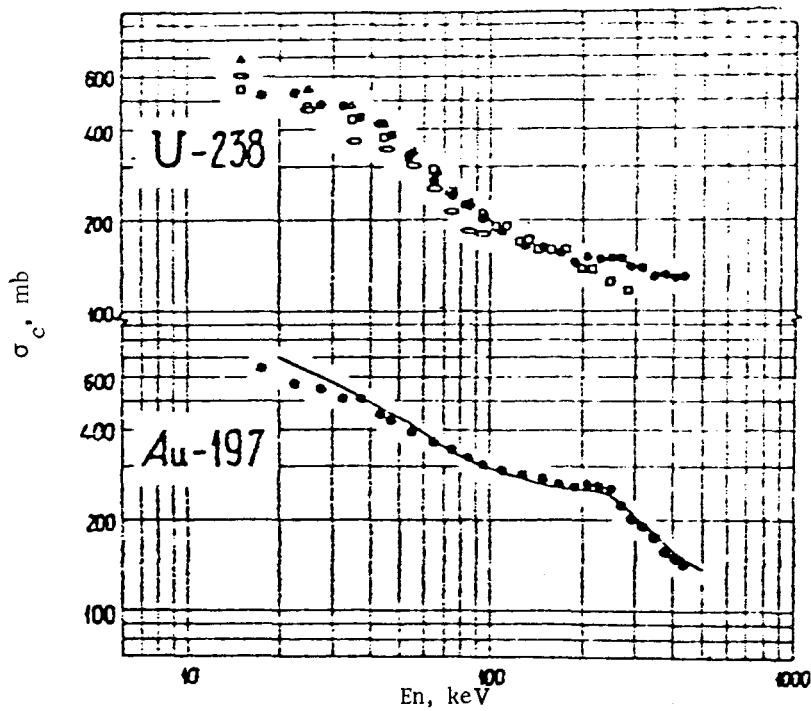


Fig. 8: Measured cross-sections for radiative capture of neutrons by  $^{238}\text{U}$  and  $^{197}\text{Au}$  nuclei; ● represents results of the present paper.